Al-TiC Composites Fabricated by a Thermally Activated Reaction Process in an Al Melt Using Al-Ti-C-CuO Powder Mixtures. Part I: Microstructural Evolution and Reaction Mechanism

YOUNG-HEE CHO, JUNG-MOO LEE, and SU-HYEON KIM

Al matrix composites reinforced with TiC particles are fabricated by a thermally activated reaction of Al-Ti-C powder mixtures in an Al melt. In the presence of CuO, reactant mixtures in the form of a pellet added to molten Al at temperatures higher than 1093 K (820 °C) instantly reach the peak temperature over 1785 K (1512 °C), followed by combustion wave propagation with *in situ* synthesizing TiC with a size of approximately 1 μm. Incomplete reaction products such as unreacted C, Al₃Ti, and TiC aggregates are also observed. The pellet microstructure evolution upon the combustion reaction indicates that preheating temperature, *i.e.*, the initial melt temperature, affects both the thermodynamic and kinetic characteristics of the reaction, and thereby influences the final microstructure of the Al/TiC composites. Based on the experimental and theoretical results, a sequence of the reaction leading upto the *in situ* synthesis of TiC is illustrated and the corresponding mechanism for the present process is proposed.

I. INTRODUCTION

Al-BASED metal matrix composites reinforced with TiC particulates have been extensively studied due to their high hardness and elastic modulus, low density, and good wettability with molten aluminum with low chemical reactivity.[1–6] TiC can be introduced to the Al matrix either by adding TiC powders directly into the melt, *i.e.*, *ex situ* process, or by an *in situ* reaction between elemental powders of Ti and C sources. In the *ex situ* process, infiltrated reinforcing TiC particles react with the Al matrix at high temperature and form a deteriorating interface layer on them and have poor wettability with the matrix due to surface contamination of the reinforcements. *In situ* TiC, on the other hand, is a thermodynamically stable phase formed by a chemical reaction and exhibits a contamination free interface with the Al matrix.[4,7–11] Among various *in situ* fabrication techniques suggested upto now, the self-propagating high temperature synthesis (SHS) developed by Merzhanov[12] is one of the most feasible and productive methods and involves ignition and self-sustaining combustion of reactants, which results in product formation.

Earlier studies adopted halide salts such as Na₃AlF₆,[13,14] KₓAlF₆,[13,14] and K₂TiF₆,[15–17] that were added to molten Al to prepare Al-Ti-C grain refiners. The use of those flux agents significantly increases the SHS reactivity, and thereby yields far more TiC *in situ* synthesized.[13,14] Moreover, it has been proposed that the fluxes addition leads to a dramatic reduction in the delay time to the SHS reaction and increases the melt over-heating temperature.[13,14] K-Al-F salts generated by the reduction of K₂TiF₆, in particular, were suggested to clean the particle surface and to remove the oxide layer from the surface of the melt, which improves the wetting of the graphite particles, promoting the formation of TiC.[17–19]

Besides shortening the SHS reaction time, lowering the temperature that initiates a combustion reaction is of importance in a low energy and cost saving *in situ* process. Our recent study reported a very practical process of SHS combined with a conventional casting to fabricate *in situ* Al/TiC composites.[20,21] It is noted that a certain amount of CuO addition thermally activates a combustion reaction of the Al-Ti-C system, and thereby enables the formation of *in situ* TiC with a large volume fraction in an Al melt at a reasonably low temperature range of 1023 K to 1193 K (750 °C to 920 °C). The microstructure evolution during SHS of Al-Ti-C, however, has not been yet clearly understood, while several mechanisms of reaction synthesis of TiC for various processes have been suggested in the literature.[7,22–29] Tong and Fang[24] employed a conventional melting process with rapid solidification for producing Al/TiC composites and reported that TiC particles are *in situ* synthesized via the following reactions:

$$[Ti] + [C] = TiC \ (s) \tag{1}$$

$$[Ti] + C \ (s) = TiC \ (s), \tag{2}$$
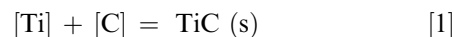
YOUNG-HEE CHO, Senior Researcher, and JUNG-MOO LEE and SU-HYEON KIM, Principal Researchers, are with the Division of Light Metals, Korea Institute of Materials Science, 797 Changwon-daero, Changwon 642-831, South Korea. Contact e-mail: jmoolee@kims.re.kr

where [Ti] and [C] are dilute solutes in liquid Al solution. Equation [1] has been proposed as dissolution-precipitation mechanism wherein either C[23] or Ti[25] solute in an Al melt migrates toward its opponent element particles with a relatively larger particle size, followed by precipitation of TiC during SHS of an Al-Ti-C powder mixture. Equation [2], on the other hand, is a solid–liquid reaction that involves the diffusion of Ti solutes in the Al melt toward a C solid phase across the solid-liquid reaction interface layer. A systematic study on the reaction mechanism based on both thermodynamics and differential thermal analysis[7] has confirmed the presence of Al_4C_3 and suggested that, along with Eqs. [1] and [2], indirect reactions are also likely to occur to synthesize TiC during heating of an Al-Ti-C preform infiltrated with molten Al as follows:

$$3Al_3Ti\ (s)\ +\ Al_4C_3(s)\ =\ 3TiC\ (s)\ +\ 13Al\ (l) \quad [3]$$

$$Al_3Ti\ (s)\ +\ C\ (s)\ =\ TiC\ (s)\ +\ 3Al\ (l) \quad [4]$$
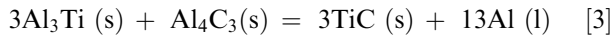
Equation (3) is further supported by Kennedy et al.[26] who suggested that TiC formation is associated with the reaction between Al_4C_3 and Al_3Ti with the evidence of differential scanning calorimetry and X-ray diffraction traces. In the study,[26] it was confirmed that TiC remains stable at temperatures above 1163 K (890 °C) where Ti dissolved in liquid Al starts to react with Al_4C_3 through the Al_3Ti dissolution as follows:

$$Al_4C_3(s) + 3[Ti]\ =\ 3TiC\ (s)\ +\ 13Al\ (l) \quad [5]$$

More recently Ding et al.[27] suggested the distribution and morphologies of TiC in Al-Ti-C master alloys are influenced by the synthesis temperature. When using a melt reaction process as reported in the study,[27] TiC aggregation is more likely to form by Eq. [5] at a melt temperature range of 1173 K to 1273 K (900 °C to 1000 °C), while TiC particles highly dispersed in the Al matrix are synthesized by Eq. [2] at 1523 K to 1573 K (1250 °C to 1300 °C).

Besides the difference in the process methods and conditions, the difference in the reaction mechanisms of TiC synthesis may arise from various initial particle sizes and powder types of an Al-Ti-C system. In this study, we aim to clarify the responsible mechanism for the *in situ* synthesis of TiC based on a systematic investigation of the microstructural evolution of an Al-Ti-C pellet mixture during the combustion reaction process recently developed. More importantly, this may suggest a key clue to minimise such undesirable features as particle agglomeration and incomplete reaction products, and thereby enables the control of the microstructure of *in situ* Al/TiC composites fabricated by the developed process.

II. EXPERIMENTAL

Al/TiC composites were prepared by adding elemental powder mixture pellets into an Al melt with a size of 400 g placed at a temperature range of 1023 K to 1193 K (750 °C to 920 °C), followed by SHS reaction. In order to make a pellet, Al (99.5 pct, ~30 μm), Ti

(99.5 pct, ~25 μm), graphite (99.999 pct, ~95 μm), and CuO (99.95 pct, ~8 μm) powders weighing a total of 40 g were mixed thoroughly at a ratio corresponding to that of stoichiometric TiC with excess Al of 1.5 mol and 0.1 mol CuO. The powder mixture was pressed into pellets in a 25-mm-diameter die under a pressure of 130 MPa, and then the pellets were placed in a preheating furnace at 473 K (200 °C) for a complete dry before adding them to an Al melt.

The powder particle size and its distribution were analyzed by a laser diffraction method. The contents of the each powder were determined by considering the molar ratio of Ti and C as to form 1 mol of TiC, as well as the volume fraction of the reinforcements. After a complete reaction, the melt was stirred for 10 minutes by rotating an impeller at 350–400 rpm so as to disperse the reaction products uniformly in it and then cast into a preheated mold. For the microstructure analysis by an optical microscopy (OM) and a scanning electron microscopy (SEM) equipped with an energy-dispersive spectrometer (EDS) samples were sectioned and prepared by standard polishing procedures with a final polishing by a 0.05 μm colloidal silica suspension. *In situ*-synthesized TiC particles of approximately 1 μm size were further analyzed by a transmission electron microscopy. Thin foil specimens for the TEM analysis were prepared by twin-jet electropolishing in a solution of 25 pct nitric acid and 75 pct methanol. Additionally, in order to further inspect the macro/microstructures of pellets, some Al-Ti-C pellets plunged in molten aluminum at the various temperatures were taken out soon after the combustion reaction. Then the pellets were vertically cross-sectioned and prepared for metallography by the procedures described as above. The size and the volume fraction of the particles were quantitatively analyzed using an image analyzer (I-solution DT).

III. RESULTS

Figure 1 shows a typical microstructure of an Al/TiC composite fabricated by the combustion reaction of a powder mixture containing carbon powder with a mean particle size of 95 μm in molten Al. Along with a large volume fraction of TiC particles (in dark gray), incomplete reaction products, such as carbon particles unreacted (in black), angular Al_3Ti phases (in light gray), and TiC clusters, are also present in the composite. *In situ* TiC with sizes less than 1 μm are well distributed throughout the Al matrix, while TiC aggregates are often found to surround unreacted carbon. The TiC agglomeration is further examined on a sample deep etched in a solution of 70 mL water and 30 mL NaOH and is presented in the inset of Figure 1.

Figure 2 shows the cross sectional microstructures of Al-Ti-C pellets taken from an Al melt soon after the SHS. It is interesting to note that the outer layer remains unreacted with containing a large volume fraction of coarse carbon in black and Al-Ti compounds, the most probably Al_3Ti. Increase in the melt temperature from 1023 K to 1193 K (750 °C to 920 °C), however, yields a far less unreacted layer and no unreacted region is

observed in the pellet processed at 1193 K (920 °C) particularly. Instead, only reacting and reacted layers are observed in the pellet and exhibit honeycomb networks of reaction products dispersed in the infiltrated Al. This suggests that the pellet after the combustion reaction becomes extremely porous, and thus the Al melt is more likely to penetrate into it, which is possibly due to the theoretical volume contraction of approximately 23.5 pct by the formation of TiC from Ti and C.

As evidenced in the pellet microstructures in Figure 2, there is a certain reaction sequence involved for the process, which was also confirmed by thermal analysis of both the pellet and melt using thermocouples types C and K, respectively.[20] Figure 3 shows time–temperature plots of both an Al-Ti-C pellet and an Al melt during the combustion reaction process that consists of three different steps: (1) preheating; (2) reaction and infiltration; and (3) reaction stabilization. In the initial stage, the pellet added to the melt is preheated during the incubation time until its temperature reaches an onset point of ignition. In the intermediate stage, the combustion reaction instantly takes place with a steep increase in the pellet temperature, followed by the Al infiltration that occurs nearly simultaneously, i.e., after 2–3 seconds of SHS. As well as the volume contraction upon synthesizing TiC, it has been suggested that improvement of the wettability of TiC particles with liquid Al by a significant increase in the temperature[30] during SHS may lead to the spontaneous Al melt infiltration into the pellet.[31] When the heat loss due to the Al infiltration exceeds the heat generation from the reaction front, however, the pellet temperature starts to
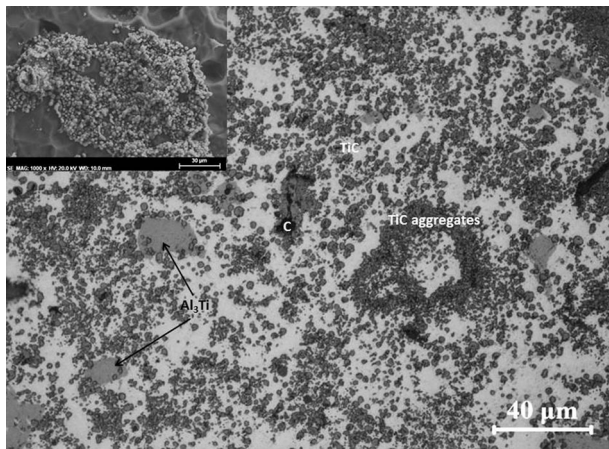

Fig. 1—OM image showing a typical microstructure of Al/TiC composites. TiC aggregates are further examined on a deep etched sample by SEM as shown in the inset.
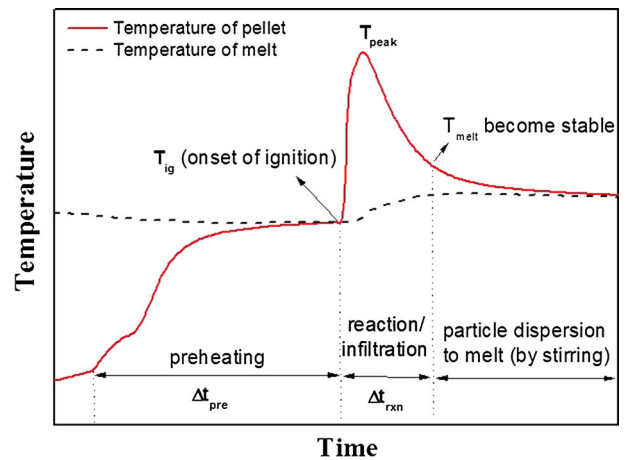

Fig. 3—Time-temperature plots of a pellet and an Al melt during the process of reaction of Al-Ti-C powder mixture containing CuO.
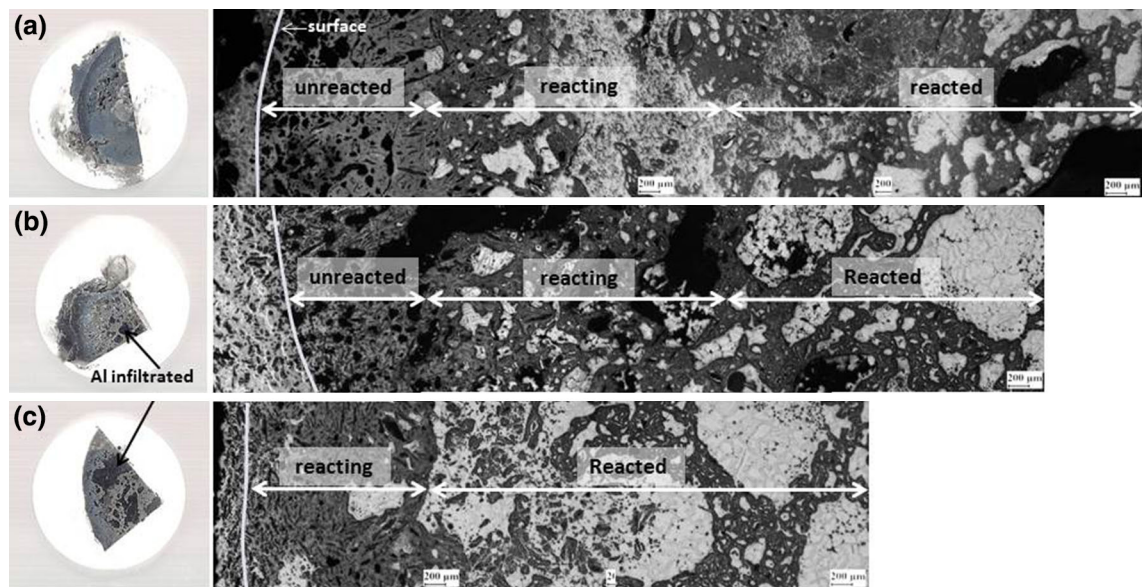

Fig. 2—OM images showing macro- and microstructures of cross-sectioned pellets plunged into an Al melt at different initial melt temperatures: (a) 1023 K (750 °C); (b) 1093 K (820 °C); and (c) 1193 K (920 °C).

decrease, slowing down or halting the combustion wave propagation. In the final stage, the pellet temperature becomes equal to the melt temperature with the reaction stabilized and then reaction products in the pellet are readily dispersed into the Al melt by mechanical stirring. The thermal analysis results generated at each melt temperature are listed in Table I.

Looking further into the microstructures in each layer of the pellets, the unreacted region mainly consists of angular Al_3Ti and unreacted C particles as shown in Figure 4, while a large volume fraction of TiC is present in the reacted region (see Figure 5). The formation of Al_2O_3 (in black) and Al_2Cu, which is associated with the decomposition of CuO, is also found along with acicular Al_3Ti phases (not presented in Figure 5) in the reacted region of the pellet as shown in Figure 5(b). In the reacting region as shown in Figure 6, TiC particles are either well dispersed in the Al infiltrated or present as aggregates which are often found adjacent to unreacted C particles. When moving toward the boundary between the unreacted and reacting layers, a large number of TiC aggregates are synthesized and the location is likely to coincide with that of angular Al_3Ti as shown in Figure 7.

The final microstructures of Al/TiC composites, which are named as melt microstructures, wherein the reaction products in the pellets are dispersed, were investigated in our earlier study.[20] Similarly to the pellet microstructures, increase in the melt temperature from 1023 K to 1193 K (750 °C to 920 °C) significantly facilitates the *in situ* synthesis of TiC. Figures 8(a) and (b) show a TEM micrograph exhibiting an *in situ*-

Table I. The Thermal Analysis Results Generated at the Initial Melt Temperature of 1023 K, 1093 K, and 1193 K (750 °C, 820 °C, and 920 °C)

Melt Temp. [K (°C)]	T_{ig} [K (°C)]	T_{peak} [K (°C)]	Δt_{pre} (s)	Δt_{rxn} (s)	Remarks
1023 (750)	1040.8 (767)	1318.8 (1045.8)	54	17	$T < 1554$ K (1281 °C) (only Eq. [2])
1093 (820)	1050.5 (777.5)	1785.9 (1512.9)	29	14	$T > 1554$ K (1281 °C) (Eqs. [1], [2])
1193 (920)	1093.2 (820.2)	2000 (1727)	10	12	$T > 1554$ K (1281 °C) (Eqs. [1], [2])

T_{ig}: ignition temperature; T_{peak}: peak temperature; Δt_{pre}: preheating time; Δt_{rxn}: reaction/infiltration time.
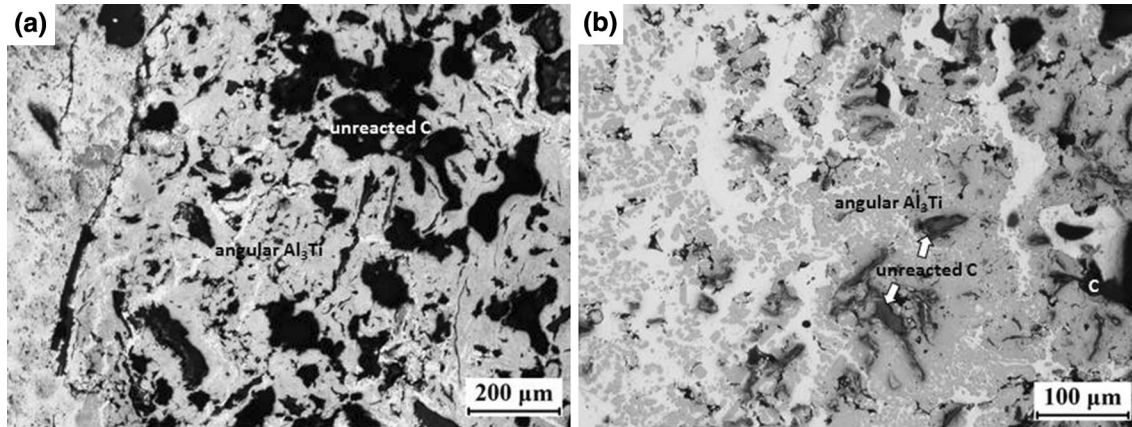

Fig. 4—OM images showing the unreacted region of the pellet processed at (*a*) 1023 K (750 °C) and (*b*) 1093 K (820 °C).
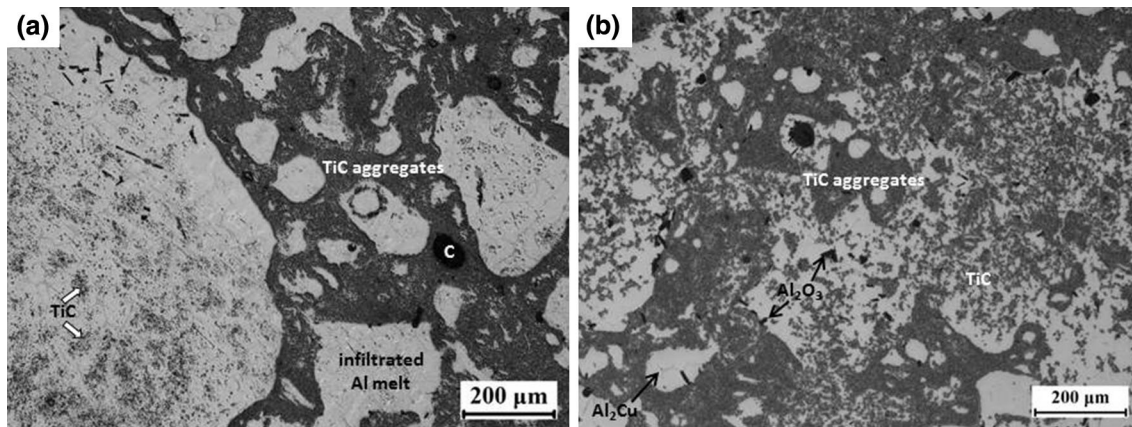

Fig. 5—OM images showing the reacted region of the pellet processed at (*a*) 1023 K (750 °C) and (*b*) 1093 K (820 °C).
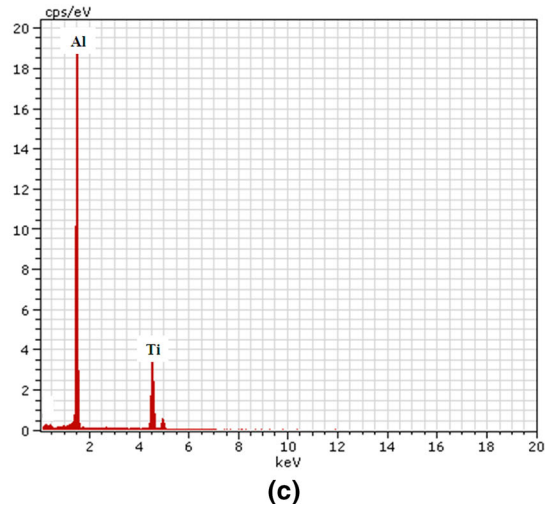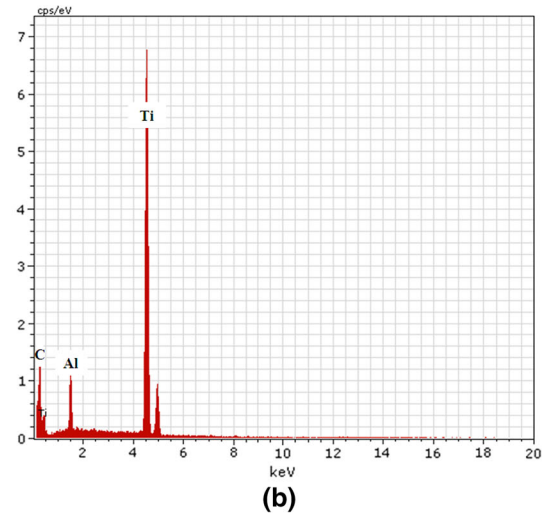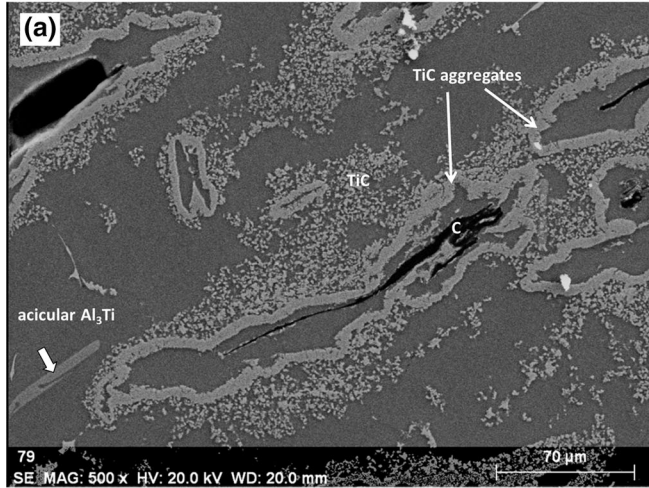
Fig. 6—(*a*) SEM image showing the reacting region of the pellet processed at 1093 K (820 °C). EDS spectra obtained from (*b*) TiC aggregates and (*c*) acicular Al₃Ti phase.
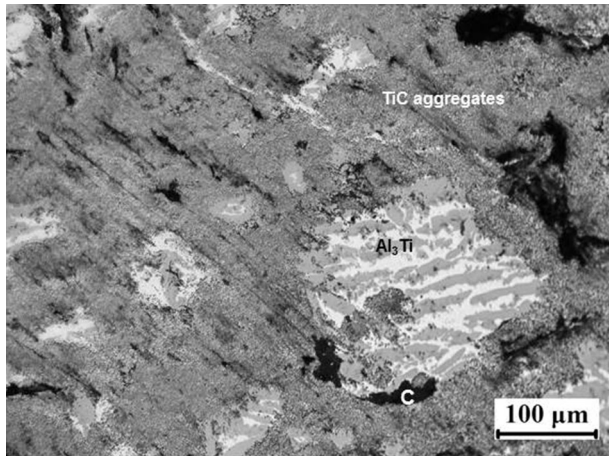

Fig. 7—OM image showing the boundary between the unreacted and reacting layers of the pellet processed at 1093 K (820 °C).

synthesized TiC (arrowed) and its corresponding EDS spectrum, respectively. The diffraction pattern obtained from the phase is also presented in the inset of Figure 8(a), which confirms that the phase is TiC (cubic, $Fm\bar{3}m$, a = 0.431 nm). It is also noted that acicular Al₃Ti is the most likely to form at 1193 K (920°C) (see Eq. [7]). This is probably due to the fact that the melt temperature increase may provide more external heat input that may facilitate local melting of Al where Ti atoms get dissolved.[7,11,26,32] For the comparison of microstructures in pellets and melts, both area fractions of each layer in the pellets and volume fractions of constituent phases in the melt are quantitatively analyzed and plotted as a function of the melt temperature in Figure 9. Increasing the melt temperature leads to an increase in the area fraction of the reacted layer in the pellet microstructure, whereas those of the unreacted and reacting layers are reduced as shown in Figure 9(a).
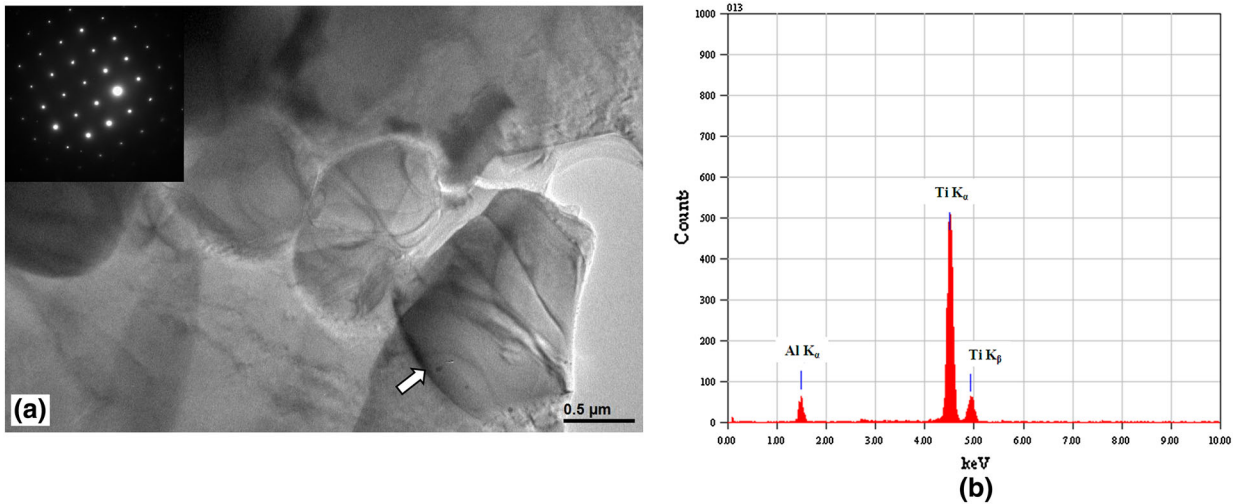
Fig. 8—(a) TEM micrograph showing *in situ*-synthesized TiC (arrowed) with its diffraction pattern presented in the inset and (b) EDS spectrum obtained from the TiC particle.
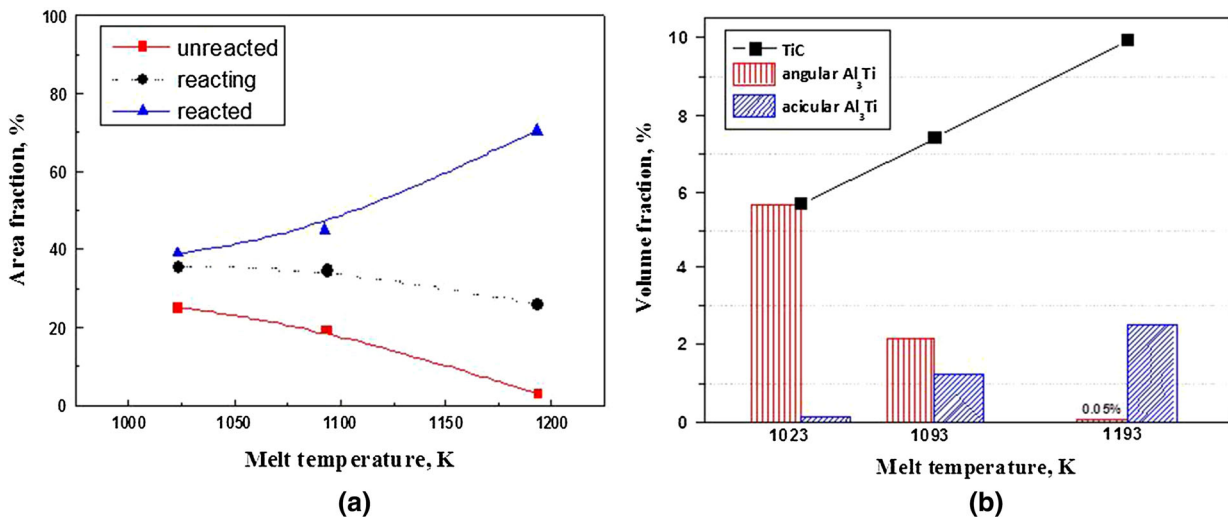

Fig. 9—(a) Area fraction of each layer in pellet microstructures and (b) volume fractions of constituent phases in melt microstructures plotted as a function of melt temperature.

This is in good agreement with the melt microstructures that exhibit a significant increase in the volume fractions of TiC and acicular Al_3Ti with producing far less angular Al_3Ti, a major constituent phase in the unreacted layer of pellets when increasing the melt temperature (Figure 9(b)).

IV. DISCUSSION

A. Thermodynamics

Combustion reaction of Al-Ti-C generally starts with ignition when the pellet mixture reaches a critical temperature by an external heat input, for instance, the melt temperature in the present work. Then serial chemical reactions occur to *in situ* synthesize TiC during the combustion wave propagation. Table II lists all the candidate reactions for the formation of TiC in the Al-Ti-C system, which all are proved to be thermodynamically stable in the processing conditions employed.[24,33] In the initial stage of the combustion reaction, a preheating stage as defined in Figure 3, the pellet temperature remains still too low to initiate the combustion reaction. Hence, along with unreacted C particles, angular Al_3Ti which are mainly present in the unreacted layer as evidenced in Figure 4, are formed by the reaction between solid Al and solid Ti as follows[7,11,26,32]:
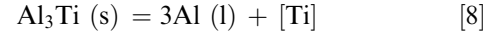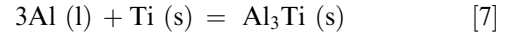
$$3Al\ (s)\ +\ Ti\ (s)\ =\ Al_3Ti\ (s) \qquad [6]$$

As the reaction proceeds, the pellet temperature exceeds the melt temperature and sharply increases upto its peak temperature after reaching the onset point of

Eq. No.	Reactions	Standard Gibbs Energy of Formation, $\Delta G°$ (J/mol)[17,25]	Remarks
[1]	[Ti] + [C] = TiC(s)	$-163382 + 80.347\,T + 0.460 \times 10 - 3\,T^2 + 3.096 \times 10^5/T - 0.962\,T\ln T$	direct reaction
[2]	[Ti] + C(s) = TiC(s)	$-91951 + 34.377\,T + 0.460 \times 10^{-3}\,T^2 + 3.096 \times 10^5/T - 0.962\,T\ln T$	direct reaction
[3]	$3Al_3Ti(s) + Al_4C_3(s) = 3TiC(s) + 13Al\,(l)$	favorable in the present work condition	indirect reaction
[4]	$Al_3Ti\,(s) + C\,(s) = TiC + 3Al\,(l)$	favorable in the present work condition	indirect reaction
[5]	$Al_4C_3(s) + 3[Ti] = 3TiC(s) + 13Al\,(l)$	favorable in the present work condition	indirect reaction
[6]	$3Al\,(s) + Ti(s) = Al_3Ti(s)$	$-4049 - 21.403\,T$	Ti source
[7]	$3Al\,(l) + Ti(s) = Al_3Ti(s)$	$-36269 + 13.115\,T$	Ti source
[8]	$Al_3Ti\,(s) = 3\,Al(l) + [Ti]$	$-60897 - 26.739\,T$	Ti source
[9]	C(s) = [C] [at T > 1554 K (1281 °C)]	$71431 - 45.97\,T$	C source
[10]	$4Al\,(l) + 3C(s) = Al_4C_3(s)$	$-268833 + 98.523\,T$	C source

ignition. Table I shows the peak temperatures experimentally analyzed during the combustion reaction of Al-Ti-C pellets, which goes upto over 1300 K (1027 °C). It is, therefore, suggested that TiC synthesis in the reacting and reacted layers are more likely to involve the direct reactions, i.e., Eqs [1] and [2], which is preceded by following reactions

$$3Al\,(l) + Ti\,(s) = Al_3Ti\,(s) \qquad [7]$$

$$Al_3Ti\,(s) = 3Al\,(l) + [Ti] \qquad [8]$$

$$C\,(s) = [C] \qquad [9]$$

$$4Al\,(l) + 3C\,(s) = Al_4C_3(s) \qquad [10]$$

Considering the thermodynamic stability of C sources, Eq. [9], in particular, takes place forward at temperatures of over 1554 K (1281 °C).[24] This importantly suggests that Eq. [1] is thermodynamically preferable because C atoms can be present as dilute solutes dissolved in liquid Al at temperatures exceeding 1554 K (1281 °C), whereas the liquid–solid reaction process, Eq. [2] is responsible for the TiC synthesis at a temperature lower than the critical temperature, i.e., 1554 K (1281 °C). TiC aggregates mainly present in the reacted layer of the pellet as evidenced in Figure 5(a) are, therefore, considered to be formed by Eq. [2] because of its relatively low peak temperature of 1319 K (1046 °C) at a melt temperature of 1023 K (750 °C). When increasing the melt temperature to 1093 K (820 °C), TiC particles well dispersed in the Al matrix are observed in the reacted and the reacting layers of the pellet as shown in Figures 5(b) and 6(a), respectively, and are suggested to form by the dissolution-precipitation process, Eq. [1], as the peak temperature reaches approximately 1785 K (1512 °C). Besides, evidence of TiC aggregates often found near unreacted C indicates that TiC formation is driven by the migration of Ti solutes in liquid Al toward the solid C when the temperature is lower than the 1554 K (1281 °C) (see Figure 6(a)). At the boundary between the unreacted and reacting layers of the pellet as shown in Figure 7, however, colonies of TiC aggregates, which are often found to surround Al_3Ti phases, suggest that the TiC formation occurs via a different reaction route, i.e., Eqs. [3] or [4] due to the temperature far below the peak temperature.

Now a question may arise regarding the presence of Al_4C_3, which has been reported to form prior to Eq. [3] that takes place at 1133 K to 1163 K (860 °C to 890 °C)[7,26] but is rarely observed in this work. Theoretical thermodynamic calculation suggests that the formation of Al_4C_3 is more favorable than that of TiC below about 1500 K (1227 °C),[34] which is supplemented by Fine and Conley[35] who reported that the formation of TiC is always stable throughout the temperature range of upto 2073 K (1800 °C), when considering the free energy of formation of both per mole of C basis. Those calculations are, however, based on 1 mol of pure solid

C equilibrated with pure solid Ti and pure solid or liquid Al and have been further corrected by Rapp and Zheng[33] who considered C (dissolved or solid), dissolved Ti and liquid Al. The calculated results predicted that TiC is thermodynamically more stable than Al_4C_3 in the temperature range of 1150 K to 1800 K (877 °C to 1527 °C) except for a very low concentration of dissolved Ti ([Ti] < 0.5 wt pct).[33] Microstructures in this study are nevertheless unlikely to confirm the direct evidence of the formation of Al_4C_3. This may suggest that Eq. [5], which involves the reaction between Al_4C_3 and [Ti], is very limited, and thus the standard Gibbs energy of TiC formation can be mainly driven by direct reactions between [Ti] and pure solid C or [C], i.e., Eqs. [1] and [2], respectively.

B. Kinetics

1. The kinetics of Al₃Ti formation

Based on the experimental results of microstructures and thermodynamic analysis, TiC synthesis mainly occurs by both the dissolution-precipitation mechanism, Eq. [1], and the solid–liquid reaction process, Eq. [2]. From a kinetic view point, it is, therefore, of importance that the decomposition of Al_3Ti into [Ti] and liquid Al via Eqs. [6] to [8] needs to proceed to get those major reactions operated. Assuming that the decomposition, Eq. [8], is much faster than the formation of Al_3Ti, Eq. [7] in particular, the overall reaction kinetics are governed by the Al_3Ti formation of which the process has been proposed to have two steps by the spherical shell model[36–38] as illustrated in Figure 10: (1) diffusion of Al to Ti through Al_3Ti layer; and (2) reaction between Al and Ti at the Al_3Ti/Ti interface. The model defines a spherical Ti particle with an initial radius of r_o that decreases to r_i as Ti is consumed to form Al_3Ti. Then the diffusion velocity of Al in the Al_3Ti layer, V_d (mol/s) can be calculated using Eq. [11],

$$V_d = 4\pi \left(\frac{D_{Al}}{\gamma_{Al}}\right)\left(\frac{\rho_{Al_3Ti}}{M_{Al_3Ti}}\right)\left(\frac{r_o r_i}{r_0 - r_i}\right)(1 - a_{Al}) \quad [11]$$

where D_{Al} is the diffusion coefficient of Al in Al_3Ti, γ_{Al} is the activity coefficient, a_{Al} is the activity of Al in
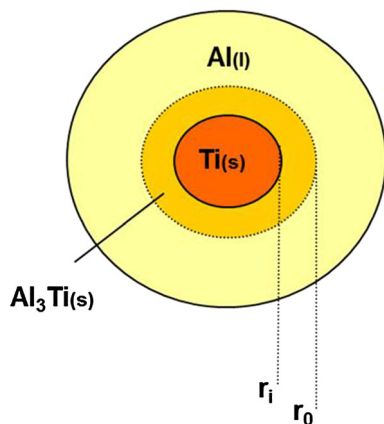

Fig. 10—A schematic diagram of the kinetic model of Al_3Ti formation during the reaction of an Al-Ti-C mixture.

Al_3Ti, ρ_{Al_3Ti}, and M_{Al_3Ti} are the density and molecular weight of Al_3Ti, respectively. When the reaction occurs following the Al diffusion, the reaction velocity, V_c (mol/s) at the Al_3Ti/Ti interface is calculated by Eq. [12],

$$V_c = \frac{4}{3}\pi r_i^2 (K_c \cdot a_{Al} - K_b), \quad [12]$$

where K_c and K_b are, respectively, the rate constants of the forward and backward reactions of Eq. [7]. Based on the law of mass conservation, both rates of the diffusion and the reaction, V_d and V_c, respectively, are equal to the overall reaction velocity, V (mol/s), which is defined as,

$$V = \frac{4\pi r_o^2}{\frac{\gamma_{Al} \cdot r_o (r_o - r_i)}{r_i \cdot D_{Al}} \cdot \left(\frac{\rho_{Al_3Ti}}{M_{Al_3Ti}}\right) + \frac{3 r_o^2}{r_i^2 \cdot K_c}} \quad [13]$$

V in Eq. [13] is also equal to the decrease rate of the Ti particle volume, V_r, which can be obtained by Eq. [14],

$$V_r = 4\pi r_i^2 \frac{\rho_{Ti}}{M_{Ti}}\frac{dr_i}{dt} \quad [14]$$

where ρ_{Ti} and M_{Ti} are the density and molecular weight of Ti, respectively. Thus the time, t, for the complete reaction of solid Ti and liquid Al to from Al_3Ti can be given by

$$t = \left(\frac{\rho_{Ti}}{M_{Ti}}\right)\left(\frac{\gamma_{Al} \cdot r_o^2}{6 D_{Al}} \cdot \frac{M_{Al_3Ti}}{\rho_{Al_3Ti}} + \frac{3 r_o}{K_c}\right) \quad [15]$$

Here, $D_{Al} = 3.82 \times 10^2 \exp(-293000/RT) \left(m^2/s\right)$ and $K_c = 5.55 \times 10^3 \exp(-125000/RT) \left(mol/m^2 s\right)$[37] are used in our calculations. Figure 9(a) shows the calculated reaction time of Al_3Ti formation as a function of Ti particle size. Considering the thermal analysis results of the total reaction time, Δt ($\Delta t = \Delta t_{pre} + \Delta t_{rxn}$), which are experimentally measured as 71, 43, and 22 s for the initial melt temperature of 1023 K, 1093 K, and 1193 K (750 °C, 820 °C, and 920 °C), respectively, (see Table I), Figure 11(a) importantly predicts the maximum particle sizes of Ti for the complete reaction. At 1023 K (750 °C), for instance, Ti particles with sizes less than 30 μm as shown in Figure 11(a) can react to form Al_3Ti, and thus the Ti powders used in the present work may not be completely reacted to form Al_3Ti due to the large mean particle size of 25 μm (Figure 11(b)), which limits the TiC formation. However, in the melt microstructure, Al_3Ti is occasionally observed with few Ti particles. This importantly suggests that the most of Al_3Ti present in the melt microstructure does not directly originate from the pellet but are formed during the mechanical stirring stage in the melt. At higher melt temperatures of 1093 K and 1193 K (820 °C and 920 °C), however, Ti with sizes upto 370 and 490 μm, respectively, (Figure 11(b)) can be associated with the complete reaction of Al_3Ti, and thereby facilitates the successive reaction of TiC.
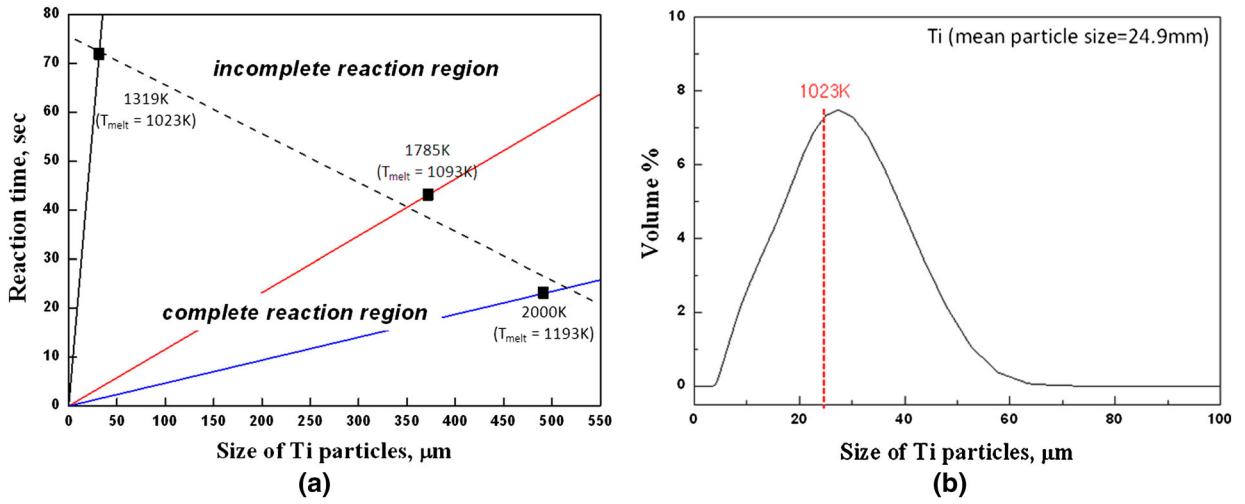
Fig. 11—(a) Reaction time calculated as a function of Ti particle size for different initial melt temperatures and (b) the size distribution of Ti powders used in the present work.
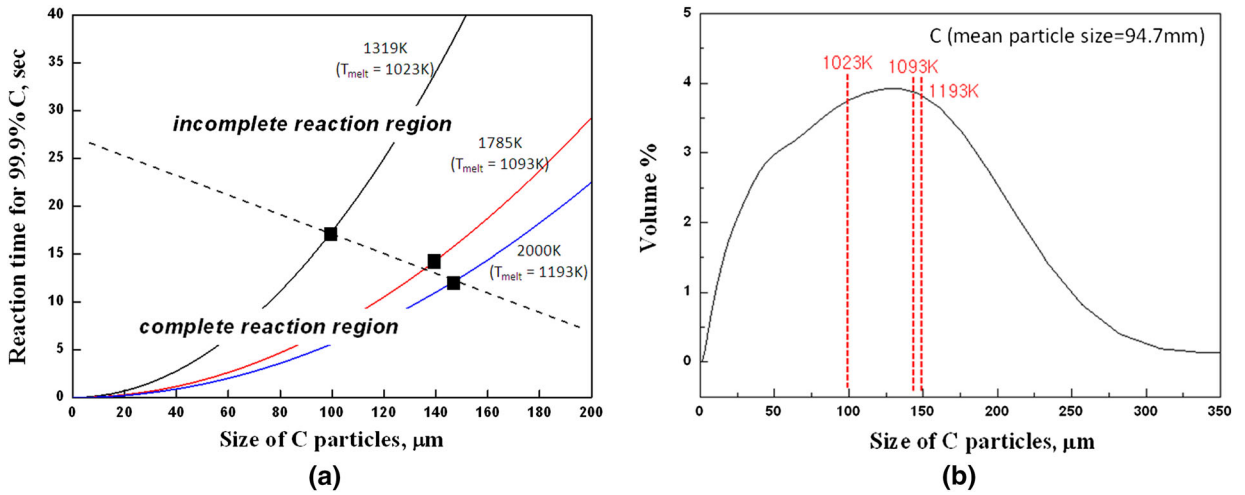

Fig. 12—(a) Reaction time calculated as a function of C particle size for different initial melt temperatures and (b) the size distribution of C powders used in the present work.

2. The kinetics of TiC formation

The reaction kinetics of TiC formation has been calculated with an assumption that the reaction rate of TiC synthesis by Eq. [1] is much faster than that by Eq. [2] which involves the diffusion process.[39,40] When employing small Ti and large C particles with mean particle sizes of 25 and 100 μm, respectively, in the present work, it is, therefore, suggested that the rate of the diffusion of Ti solutes in the Al matrix toward C is the controlling step of the TiC synthesis. Based on the stoichiometry of Eq. [2] and the spherical particle model,[39] the molar diffusion rate of Ti across the intermediate reaction layer in the Al melt to the C surface can be equal to the carbon molar consumption rate, which can be defined as

$$\frac{dV}{dt} = \frac{-\pi D \left(\frac{1+2\beta}{\beta}\right) \left(\frac{6}{\pi}\right)^{1/3} \cdot N_c^{2/3} \cdot V^{4/3}}{N_{Al} \cdot \frac{M_{Al}}{\rho_{Al}} + \frac{\rho_c}{M_c} \cdot \frac{M_{Ti}}{\rho_{Ti}} \cdot V} \quad [16]$$

in units of (m^3/mol s). In Eq. [16], V = $N_c \pi d p^3/6$ is the total volume of C, D is the coefficient of Ti diffusion in Al, N_{Al} is the total moles of Al divided by the total number of C particles, N_c in the initial powder mixture, and β is the thickness of the reaction layer divided by the instantaneous diameter of the C particle, d_p.

The time for 99.9 pct of the molar volume consumption of the C particle during the TiC synthesis can be calculated from

$$t = \left(\frac{10^3}{2} \cdot N_{Al} \cdot \frac{M_{Al}}{\rho_{Al}} \cdot \frac{\rho_c}{M_c} + \frac{1}{6} \cdot \frac{\rho_c}{M_c} \cdot \frac{M_{Ti}}{\rho_{Ti}}\right) \cdot \left(\frac{\beta}{1+2\beta}\right) \cdot \frac{d_0^2}{D} \quad [17]$$

where d_0 is the initial particle size of C when $t = 0$. In this study, $N_{Al} = 1.5$ mol, $D = 3.90 \times 10^{-7} \exp(-40.2/RT)$ (m/s^2), and $\beta = 0.02$ were used.[40] Figure 12(a) exhibits the calculated reaction time for 99.9 pct C consump-
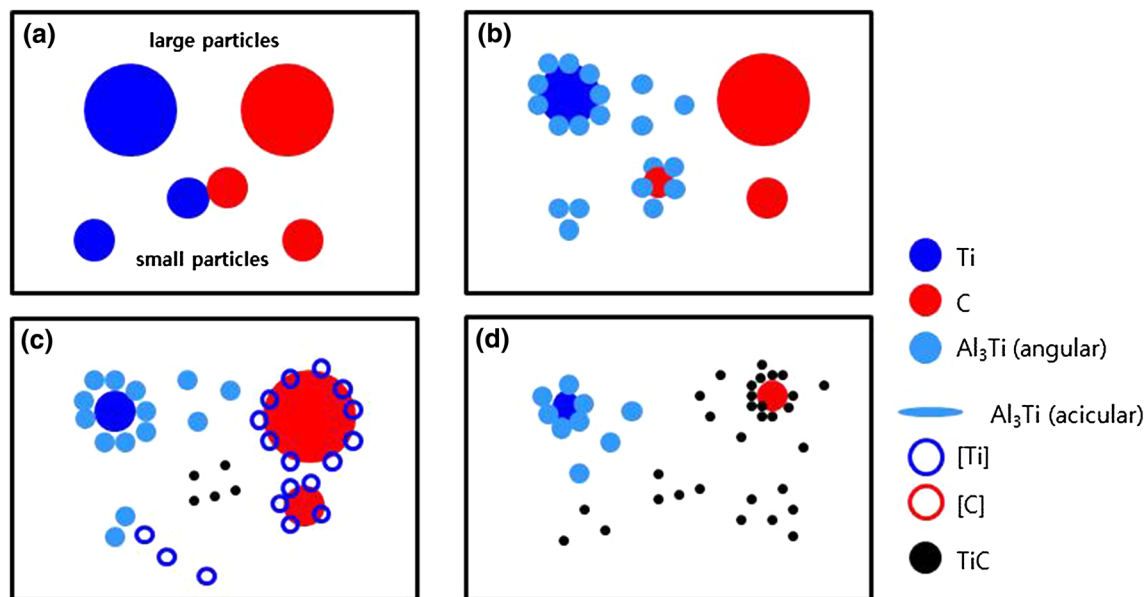
Fig. 13—A schematic illustration showing the reaction mechanism at a lower temperature condition.

tion as a function of C particle size along with the measured time, Δt_{rxn} for different initial melt temperatures. Considering that C particle can be completely converted into TiC during the reaction time of 17, 14, and 12 s by increasing the peak temperature to 1319 K, 1785 K, and 2000 K (1046 °C, 1512 °C, and 1727 °C), respectively (see Table I), the maximum size of C particles at each initial temperature of the melt can be predicted as denoted in Figure 12(a). It is noted that C particles with sizes up to approximately 150 μm are expected to react thoroughly as increasing the melt temperature up to 1193 K (920 °C). However, unreacted C particles that are often observed in the final microstructure is probably due the broad size distribution of the C powder used in this study as shown in Figure 12(b). Large C particles with sizes of over 150 μm are, therefore, likely to remain unreacted even at a peak temperature of 2000 K (1727 °C).

C. Sequence of Microstructural Evolution

Figures 13 and 14, respectively, illustrate the reaction mechanisms responsible for the *in situ* synthesis of TiC in the low and high temperature conditions (1023 K and 1093 K (750 °C and 820 °C), respectively) employed in the present process. Firstly, if Ti and C particles with both large and small sizes are present in an Al melt at lower temperature (Figure 13(a)), Ti particles are surrounded with angular Al$_3$Ti phases (Eqs. [6] and [7]) in the initial stage. A small C particle that is in direct contact with Ti is also surrounded with Al$_3$Ti as shown in Figure 13(b) and then starts to react to form TiC by Eq. [4] (see Figure 13(c)). In this stage, Al$_3$Ti phases are decomposed into [Ti] in the Al melt by Eq. [8], followed by diffusion of the solutes toward the surface of C particles. Finally the diffused [Ti] reacts with the solid C to form TiC by Eq. [2], while the large C is unlikely to be completely reacted and is rather surrounded with TiC

aggregates as shown in Figure 13(d). In a similar way, the large Ti particle that remains incompletely reacted ends up being surrounded with angular Al$_3$Ti phases (Figure 13(d)). This is in good agreement with the final microstructure obtained from the melt temperature of 1023 K (750 °C) (see Figure 15(a)). The reaction mechanism suggested for the lower temperature condition may also account for the microstructure evolution in the unreacted or reacting regions of a pellet or in a case of low CuO content (*e.g.*, 0.03 mol in the present work).

Similarly to the lower temperature conditions, if there are Ti and C particles with both large and small sizes in the Al matrix (Figure 14(a)) at a high temperature condition of 1193 K (920 °C), a large Ti particle is surrounded with angular Al$_3$Ti phases, while a small Ti adjacent to C also forms Al$_3$Ti phases that are likely to envelop the C particle as shown in Figure 14(b). Then the C particle surrounded with Al$_3$Ti starts to react to form TiC by Eq. [4] and Al$_3$Ti away from C sources are decomposed into [Ti] solutes in the Al melt by Eq. [8]. In such higher temperature conditions as a high initial melt temperature or high content of CuO addition (*e.g.*, 0.2 mol CuO in the present work), moreover, C particles are also likely to get dissolved into [C] in this stage (see Figure 14(c)) by Eq. [9] possibly due to a high temperature that exceeds 1554 K (1281 °C) during the reaction. Ti and C with smaller initial sizes are now present as [Ti] and [C], respectively, which instantly drives them to synthesize TiC by Eq. [1]. In the meantime, [Ti] solutes are also likely to diffuse to a large C particle to form TiC by Eq. [2] and [C] solutes diffuse toward [Ti] decomposed from the Al$_3$Ti particles to form TiC (Figures 14(d) and (e)). In the final stage of the reaction as shown in Figure 14(f), along with a large volume fraction of TiC, the large C particle that remains incompletely reacted is often surrounded by TiC. This may interfere with further diffusion of [Ti] to the large C and hence leads to excess Ti localized in the Al melt,
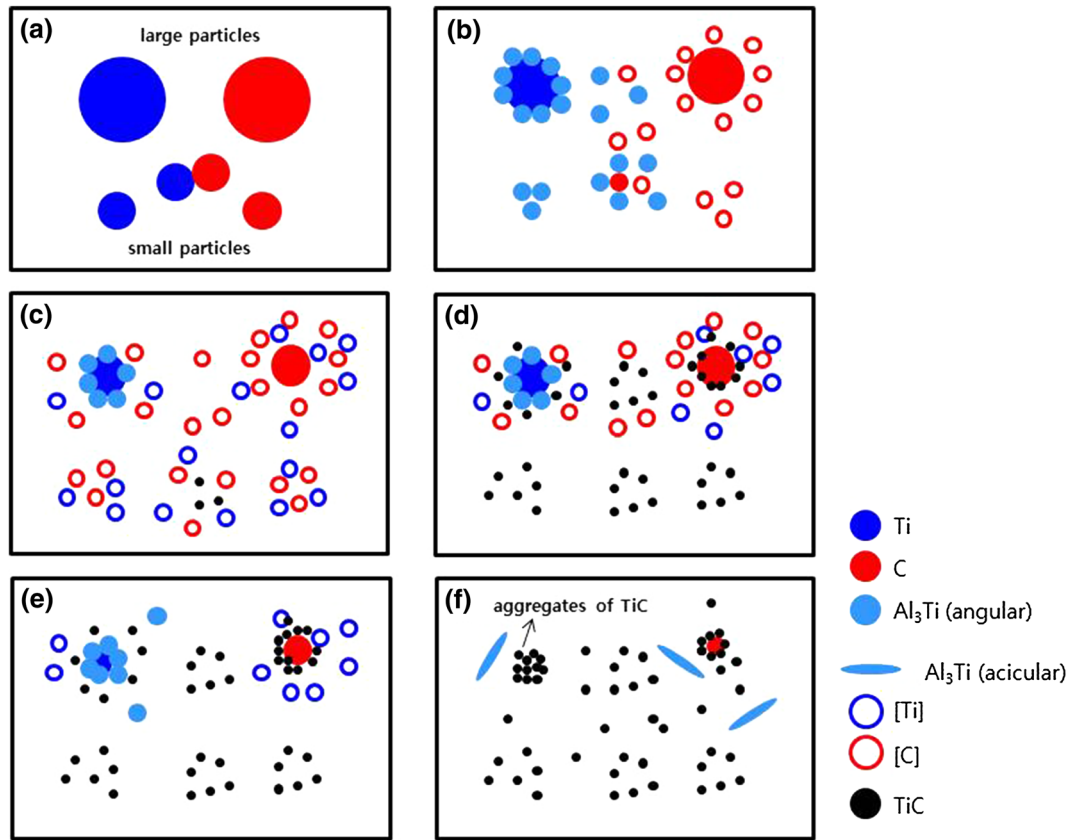
Fig. 14—A schematic illustration showing the reaction mechanism at a higher temperature condition.
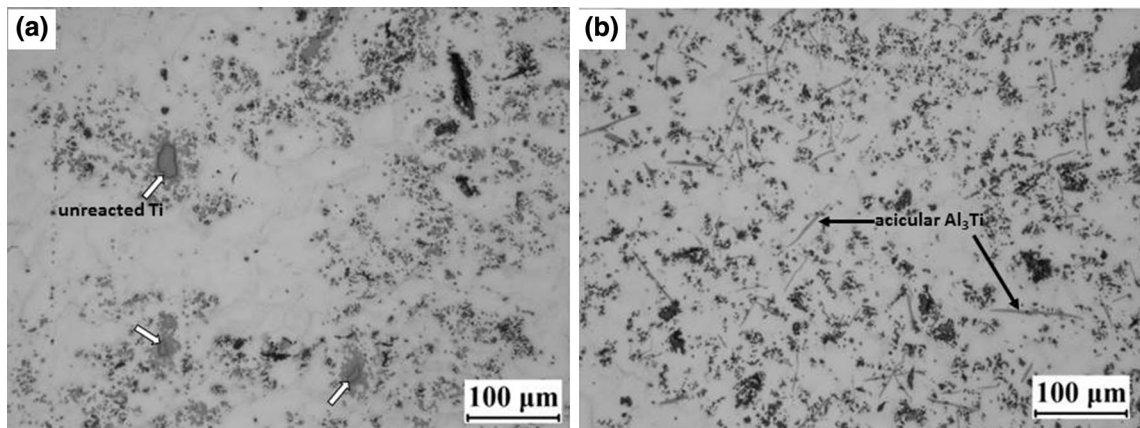

Fig. 15—Optical micrographs showing the final microstructure obtained from the melt temperature of (a) 1023 K (750 °C) and (b) 1193 K (920 °C).

followed by the formation of acicular Al_3Ti upon solidification. The large size Ti, on the other hand, is thoroughly consumed to form TiC via Eq. [8] followed by Eq. [1], but occasionally leaves TiC aggregates behind (Figure 14(f)). This well agrees with the final microstructure obtained from the initial melt temperature of 1193 K (920 °C) as shown in Figure 13(b). Based on the suggested reaction mechanism, the microstructure control of Al/TiC composites is now in progress and is to be further discussed in our future study that

will present the mechanical properties for the enhanced performance.

V. CONCLUSIONS

Al/TiC composites were fabricated by immersing a pellet of Al-Ti-C-CuO powder mixture into an Al melt at a temperature range of 1023 K to 1193 K (750 °C to 920 °C), followed by a self-sustaining combustion reac-

tion. *In situ*-synthesized TiC particles with a size of approximately 1 μm were well distributed in the final microstructure along with incomplete reaction products, such as carbon particles unreacted, polygonal-shaped Al$_3$Ti phases and TiC agglomerates. The polygonal-shaped Al$_3$Ti phases mainly originated from the unreacted pellet layer that forms while the pellet is heated upto ignite and their volume fraction can be significantly reduced by accelerating SHS by increasing the initial melt temperature. Besides the melt temperature, the sizes of elemental powders are of importance and play a key role in controlling the microstructure of the *in situ* Al/TiC composites. Both Ti and C with large particle sizes are less likely to react completely to form TiC and are also associated with the formation of TiC aggregates even in the higher temperature condition provided in the developed process.

REFERENCES

1. X.C. Tong and H.S. Fang: *Metall. Mater. Trans. A*, 1998, vol. 29A, pp. 893–902.
2. P. Sahoo and M.J. Koczak: *Mater. Sci. Eng., A*, 1991, vol. A131, pp. 69–76.
3. I. Gotman, M.J. Koczak, and E. Shtessel: *Mater. Sci. Eng., A*, 1994, vol. A187, pp. 189–199.
4. H. Nakata, T. Choh, and N. Kanetake: *J. Mater. Sci.*, 1995, vol. 30, pp. 1719–27.
5. Y.F. Liang, J.E. Zhou, and S.Q. Dong: *Mater. Sci. Eng., A*, 2010, vol. 527, pp. 7955–60.
6. X.C. Tong and A.K. Chosh: *J. Mater. Sci.*, 2001, vol. 36, pp. 4059–69.
7. T. Nukami and M.C. Flemings: *Metall. Mater. Trans. A*, 1995, vol. 26A, pp. 1877–84.
8. M.K. Premkumar and M.G. Chu: *Mater. Sci. Eng., A*, 1995, vol. A202, pp. 172–78.
9. X.C. Tong: *J. Mater. Sci.*, 1998, vol. 33, pp. 5365–74.
10. A.E.W. Jarfors, L. Svendsen, M. Wallinder, and H. Fredriksson: *Metall. Trans. A*, 1993, vol. 24A, pp. 2577–83.
11. B. Yang, G. Chen, and J. Zhang: *Mater. Des.*, 2001, vol. 22, pp. 645–50.
12. A.G. Merzhanov: *J. Mater. Process. Technol.*, 1996, vol. 56, pp. 222–41.
13. P. Li, E.G. Kandalova, V.I. Nikitin, A.G. Makarenko, A.R. Luts, and Y. Zhang: *Scripta Mater.*, 2003, vol. 49, pp. 699–703.
14. P. Li, E.G. Kandalova, and V.I. Nikitin: *Mater. Lett.*, 2005, vol. 59, pp. 2545–48.
15. G.S. Vinod Kumar, B.S. Murty, and M. Chakraborty: *J. Alloys Compd.*, 2005, vol. 396, pp. 143–50.
16. R. Bauri: *Trans. Indian Inst. Met.*, 2009, vol. 62, pp. 391 95.
17. Y. Birol: *J. Alloys Compd.*, 2008, vol. 454, pp. 110–17.
18. V.H. López and A.R. Kennedy: *J. Colloid Interface Sci.*, 2006, vol. 298, pp. 356–62.
19. Y. Mazaheri, M. Meratian, R. Emadi, and A.R. Najarian: *Mater. Sci. Eng., A*, 2013, vol. 560, pp. 278–87.
20. Y.-H. Cho, J.-M. Lee, H.-J. Kim, J.-J. Kim, and S.-H. Kim: *Met. Mater. Int.*, 2012, vol. 19, pp. 1109–16.
21. Y.-H. Cho, J.-M. Lee, H.-J. Kim, J.-J. Kim, and S.-H. Kim: *Proc 13th Int Conf Alum Alloys*, 2012. pp. 201–06.
22. W.-C. Lee and S.-L. Chung: *J. Am. Ceram. Soc.*, 1997, vol. 80, pp. 53–61.
23. G. Xiao, Q. Fan, G. Meizhuan, and Z. Jin: *Mater. Sci. Eng., A*, 2006, vol. 425, pp. 318–25.
24. X.C. Tong and H.S. Fang: *Metall. Mater. Trans. A*, 1998, vol. 29A, pp. 875–91.
25. E. Zhang, S. Zeng, B. Yang, Q. Li, and M. Ma: *Metall. Mater. Trans. A*, 1999, vol. 30A, pp. 1147–51.
26. A.R. Kennedy, D.P. Weston, M.I. Jones, and C. Enel: *Scripta Mater.*, 2000, vol. 42, pp. 1187–92.
27. H. Ding, X. Liu, Y. Lina, and G. Zhao: *Scripta Mater.*, 2007, vol. 57, pp. 575–78.
28. Y. Choi and S.-W. Rhee: *J. Am. Ceram. Soc.*, 1995, vol. 78, pp. 986–92.
29. Z. Wang, X. Liu, J. Zhang, and X. Bian: *J. Mater. Sci. Lett.*, 2003, vol. 22, pp. 1427–29.
30. A. Contreras, C.A. Leon, R.A.L. Drew, and E. Bedolla: *Scripta Mater.*, 2003, vol. 48, pp. 1625–30.
31. J. Zhang, J.-M. Lee, Y.-H. Cho, S.-H. Kim, and Y. Huashun: *Scripta Mater.*, 2013, vol. 69, pp. 45–48.
32. M.S. Song, B. Huang, M.X. Zhang, and J.G. Li: *Int. J. Refract. Met. Hard Mater.*, 2009, vol. 27, pp. 584–89.
33. R.A. Rapp and X. Zheng: *Metall. Trans. A*, 1991, vol. 22A, pp. 3071–75.
34. A. Banerji and W. Reif: *Metall. Trans. A*, 1986, vol. 17A, pp. 2127–37.
35. M.E. Fine and J.G. Conley: *Metall. Trans. A*, 1990, vol. 21A, pp. 2609–10.
36. A. Hibino and R. Watanabe: *J. Jpn. Inst. Met.*, 1991, vol. 55, pp. 1256–62.
37. T. Matsubara, K. Uenishi, and K.F. Kobayashi: *Mater. Trans., JIM*, 2000, vol. 41, pp. 631–34.
38. J.-M. Lee, S.-B. Kang, T. Sato, H. Tezuka, and A. Kamio: *Mater. Sci. Eng., A*, 2003, vol. A343, pp. 199–209.
39. A.M. Kanury: *Metall. Trans. A*, 1992, vol. 23A, pp. 2349 56.
40. E. Zhang, S. Zeng, B. Yang, Q. Li, and M. Ma: *Metall. Mater. Trans. A*, 1999, vol. 30A, pp. 1153–57.